




e-ISSN: 2618-575X

INTERNATIONAL ADVANCED RESEARCHES  
and  
ENGINEERING JOURNAL

Journal homepage: [www.dergipark.org.tr/en/pub/iarej](http://www.dergipark.org.tr/en/pub/iarej)International  
Open Access Volume 08  
Issue 01

April, 2024

**Research Article****Failure analysis of cast iron housing unit of UCF-216 type ball bearing****Mustafa Guven Gok**<sup>a,\*</sup>  and **Mehmet Bunyamin Sahin**<sup>b</sup> <sup>a</sup>Department of Metallurgical and Materials Engineering, Gaziantep University, 27310, Gaziantep, Turkey<sup>b</sup>(Student) Department of Metallurgical and Materials Engineering, Gaziantep University, 27310, Gaziantep, Turkey

## ARTICLE INFO

*Article history:*

Received 08 June 2023

Accepted 19 February 2024

Published 20 April 2024

*Keywords:*

Casting defect

Failure analysis

Finite element analysis

Stress

## ABSTRACT

One of the most common problems faced by briquette machine users in the industry is the failure of the cast iron housing unit of the UCF-216 bearings, to which the main shaft of the briquette machine is attached. In this study, the failure mechanism of a cast iron housing unit of a UCF-216 bearing broken during operation in a briquette machine was analyzed in order to develop a solution to the problem. Failure was occurring in the bolt hole areas of the housing unit. First of all, spectral analysis was performed and it was determined that the housing unit was grey cast iron. Then, the macrostructures of both unused and damaged housing units were examined. Some casting defects were detected in the bolt hole areas of the unused housing unit. It was also learned that during the assembly of the UCF-216 to the briquette machine, no torque meter was used while the bolts were tightened. In order to understand the effect of possible overtightening of the bolts, the system was modelled as a 3D solid. This model was exported to the finite element software and different bolt pretensions were applied considering the stresses created by the bolt tightening forces on the housing unit. As a result, it was understood that if the ratio of the stress caused by the axial bolt tightening force in the UCF-216 bearing unit to the yield stress of the UCF-216 housing unit is above 50%, fatigue failure will occur.

**1. Introduction**

Concrete building block machines (CBBM) have been called by different names such as briquette machine, bims (pumice) machine, pumice machine and block making machine in the construction industry. This name difference is due to the purpose of using the CBBM. Because with the same machine, different products could be produced. By using several molds in the CBBM, construction materials with variable properties and dimensions such as interlocking briquettes, curbstones, hollow concrete blocks and pumice blocks can be produced. The most basic task of the CBBM is to shape the construction material in different molds using vibration and pressure. Actually, a CBBM is a kind of mass production machine. Because in this machine, which generally has an automation system, pumice, cement and water mixture in certain proportions is taken into molds and compressed with the help of vibration and hydraulic press [1–4].

The development of a CBBM with movable, adjustable dies that could make solid blocks dates back to the early 1900s. Harmon S. Palmer's "Machine for Molding Hollow Concrete Building Blocks" was patented in 1902 and made

a significant contribution to the development of the CBBMs known today [5,6]. Due to the fact that the construction materials produced in CBBMs have affordable prices, desired quality and repeatable features, these machines attract great attention on a global scale. Today, CBBMs are produced in both industrialized and developing countries. Türkiye is one of the important CBBM manufacturers and a significant part of the machines produced in Türkiye has been exported.

The CBBMs can be divided into 3 different categories as manual, semi-automatic and fully automatic. In addition, there are many types and models of CBBMs with different capacities. Molds can be produced and mounted according to the desired size and model for the product to be produced in the CBBM. The latest models of these machines usually consist of different basic parts, namely the main body, the picking robot, the belt separator, the elevator and other mechanisms. All of the CBBMs work with electrical energy, and semi and fully automatic machines are controlled by automation software. The upper rammer, which is an important part of the CBBM and located on the main body of the machine, allows the

\* Corresponding author. Tel.: +90 (342) 360 1200.

E-mail addresses: [mnggok@gantep.edu.tr](mailto:mnggok@gantep.edu.tr) (Mustafa Guven Gok), [mehmetbunyaminsahin27@gmail.com](mailto:mehmetbunyaminsahin27@gmail.com) (Mehmet Bunyamin Sahin)

ORCID: 0000-0002-5959-0549 (Mustafa Guven Gok), 0009-0007-2401-836X (Mehmet Bunyamin Sahin)

DOI: [10.35860/iarej.1311569](https://doi.org/10.35860/iarej.1311569)© 2024, The Author(s). This article is licensed under the CC BY-NC 4.0 International License (<https://creativecommons.org/licenses/by-nc/4.0/>).

arms to move the compression mold upwards. The arms are fixed to the main shaft on the main body of machine and this main shaft is connected to the machine body by means of UCF type bearings so that it can rotate around its own axis (see Figure 1). The UCF type bearings are fixed to the machine body with M22 or M23 bolts and nuts. Since there are 2 main shafts for the mold holding arms, 4 UCF type bearings are used in a machine [7]. However, it is reported that UCF type bearings are suddenly broken while working on the CBBM as a very frequent problem.

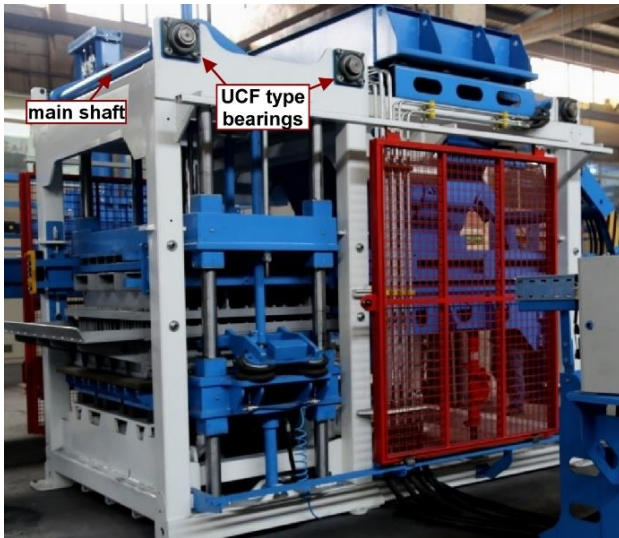


Figure 1. Main shaft and UCF type bearings on a fully automatic CBBM

The UCF series bearings are a square flange bearing type with four fixing holes and have a wide inner ring insert. Ball bearing units have international coding. The UCF coding on the housing unit used in this study indicates that the housing unit has a square flange type and cylindrical bore. The shaft diameter is coded in the numbers after UCF (UCF-216). Here the first digit is the diameter series of the bearing and the other digits are the size code of the bearing bore. They are one of the most

preferred machine elements in the industry and have different codes according to their sizes. The UCF serial bearings consist of 2 main parts, a bearing and a cast iron housing. There is no doubt that the class and therefore the quality of the cast iron material that makes up the body (housing unit) of the UCF will vary according to the manufacturer [8–10]. In this study, the cast iron housing unit of the UCF-216 bearing, which was damaged during operation in the CBBM, was analyzed. Therefore, the aim of this study is to analyze the failure mechanism in the UCF-216 bearing housing unit, which is used in CBBMs and is damaged (broken) during operation, and to develop suggestions for solving the failure problem.

## 2. Material and Methods

### 2.1. Definition of failure

Basically, the problem was that the cast iron housing unit of the UCF-216 type ball bearings used in a fully automatic CBBM were broken. It was reported that the housing unit of the UCF-216 was damaged after the CBBM was used for a very short time. Moreover, the same problem was experienced both in the newly produced CBBM and after the replacement of the broken UCF-216 with a new one. The housing unit of the UCF-216 was made of cast iron. The UCF-216 housing unit was designed and produced in such a way that no damage would occur as a result of the load during operation under ideal conditions, and it had an infinite fatigue life. However, contrary to this situation, it was broken very often. The most important data we had was that the bolts were tightened without using a torque meter during the assembly of the UCF-216 to the CBBM. In order to understand and solve the problem, as explained in the next sections, both UCF-216 housing units were investigated macrostructurally and different bolt tightening scenarios were created in finite element software.

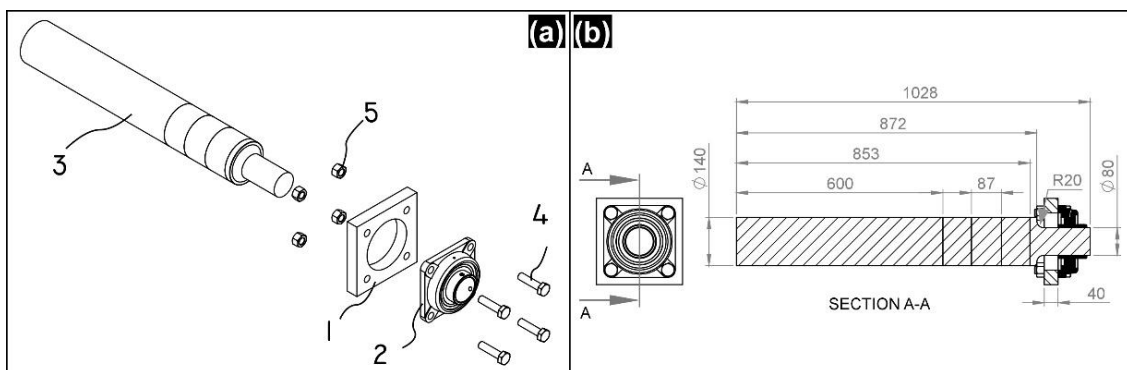


Figure 2. (a) Exploded 3D view of UCF and main shaft, (b) 2D technical drawing of the system.

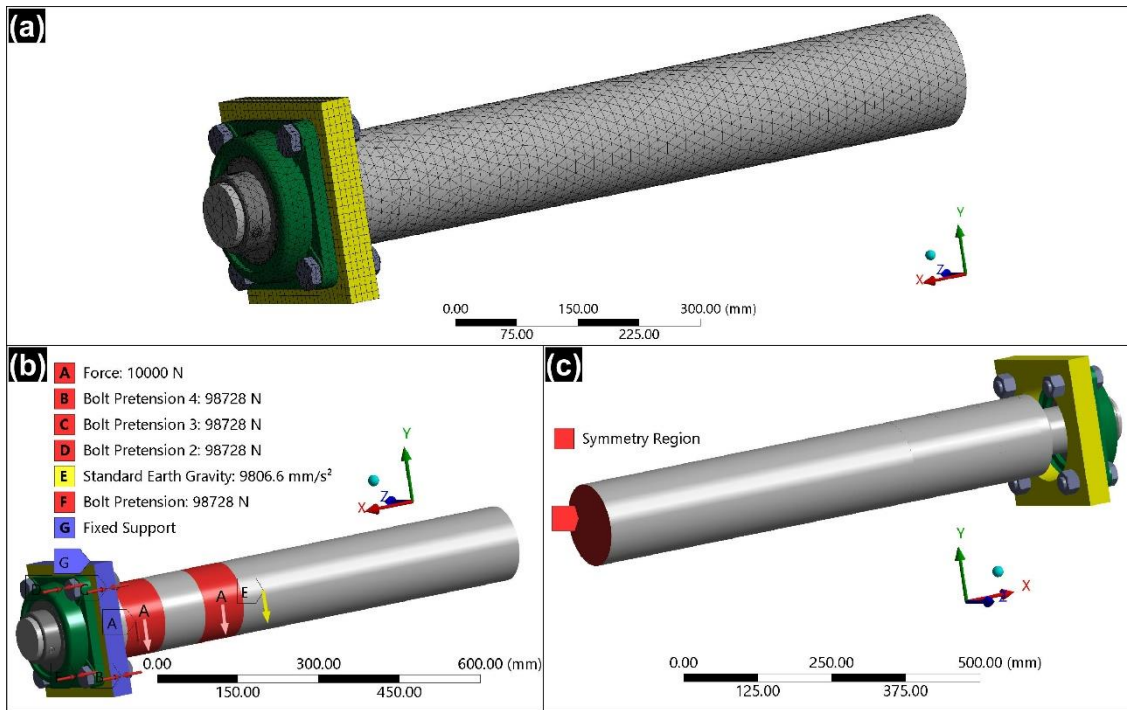


Figure 3. (a) finite element model showing mesh elements, (b) loading and (c) symmetry conditions of the system.

## 2.2. Modelling of parts

For analysis, the 3D assembly diagram and 2D technical drawing of the system created according to the actual conditions and dimensions in the CBBM were given in Figure 2 (a) and (b), respectively.

SolidWorks software was used for the technical drawings and solid modelling of the parts of the system. The system consisted of five basic components. Parts 1, 2, 3, 4 and 5 shown in Figure 2 (a) were the headstock, UCF-216 bearing (with all its components), main arm, bolts and nuts, respectively. The UCF-216 (part number 2) consisted of a housing unit (made of cast iron) with 4 bolt holes for mounting and ball bearing system parts. Actually, the headstock (part number 1) was the body of the CBBM. In this part (part number 1), there were 4 bolt holes for mounting the UCF-216 (part number 2) and a hole in the middle to allow the main arm (part number 3) to pass contactless. The housing unit of UCF-216 (part number 2) was mounted to the headstock (part number 1) with 4 pieces M22 bolts (part number 4) and nuts (part number 5). Thanks to the bearing in the UCF-216, the main arm could rotate freely on its own axis. Thickness of the headstock was 40 mm. The diameter of the main arm mounted on the UCF-216 was 80 mm, while the diameter of the other part was 140 mm.

## 2.3. Spectral analysis of UCF-216

Spectral analysis was performed to determine the chemical composition of the UCF-216 housing unit. For this, an Oxford Instruments Foundry-Master Pro optical emission spectrometer was used. According to the spectral

analysis results given as chemical composition in Table 1, the UCF-216 housing unit was made of grey cast iron. It is already stated in the catalogs of bearing manufacturing companies that UCF series bearing bodies are produced from gray cast iron material.

## 2.4. Numerical model, material, meshing, contact and boundary conditions

The 3D solid model of the system, which was created in accordance with its real dimensions and design using SolidWorks software, was exported to Ansys Workbench software. The material properties were defined as having linear elastic properties. On the other hand, it was very difficult or even impossible to define exact mechanical property values for cast irons. Because too many elements in the chemical composition of cast iron and the fact that they can be added to the composition in a wide range seriously affect its mechanical properties. In addition, especially the amount of graphite has a great effect on the stress-strain curve. While the tensile strength of grey cast irons was generally between 100 and 350 MPa, their compressive strength could be 3-4 times higher [11–13]. Therefore, in this study, consistent with studies in the literature [14–16], density, yield strength, ultimate strength, Young's modulus and Poisson's ratio values for grey cast iron were chosen as 7.1 g/cm<sup>3</sup>, 328 MPa, 480 MPa, 144.7 GPa and 0.28, respectively, since exact values must be defined in the software. As given in previous study [17], properties of AISI4140 steel were defined for bolts and nuts, and mechanical properties of structural steel were defined for other parts.

Table 1. Chemical composition (wt. %).

Fe	C	Si	Mn	Cu	Ti	P	S	Bi	Cr	Ni	Mo	Others
93.0	3.77	2.26	0.541	0.116	0.096	0.091	0.077	0.016	0.01	0.005	0.002	0.016

After the material definition, the contact zones between neighboring components were determined. The contact surface of the UCF-216 housing unit with the headstock was defined as frictional (friction coefficient of 0.15  $\mu$ ). As seen in Figure 3 (a), tetrahedron and hexahedral meshes were used to divide the system into finite elements. Different body sizing operations were applied to parts of the system in order to increase the mesh quality by approximating the mesh size distribution. As a result of the meshing process, the system contained a total of 174303 nodes and 107536 elements. In this study, the failure analysis of the housing unit of an UCF-216 bearing used in the CBBM was made. For this, as seen in Figure 3 (b), it has been determined that the maximum force acting on the UCF-216 by means of the main arm (part number 3) is 10000 N. The load was applied to the arm from two regions on the arm and in the -Y direction. These regions were the real places on the machine where the gripper arms were located and therefore the load was affected. On the other hand, the entire cross-sectional surface of the headstock was set as fixed support and a standard earth gravity in the -Y direction was applied to the entire system (see Figure 3 (b)). On the other hand, as the system is connected to the CBBM from the other side of the arm under the same conditions, as seen in Figure 3 (c), the cross-sectional surface of the midpoint of the arm length was defined as the symmetry region. Also, different bolt pretensions were applied to the bolts in order to see the effect of the bolt tightening force, since the UCF-216 was not assembled to the headstock with a torque meter. The stresses created by the axial bolt clamping force (ABCF) on the housing unit of UCF-216 ( $\sigma_{ABCF}$ ) were taken into account when calculating the bolt pretensions.

For this, using Equation 1, bolt pretensions were applied to the bolts to create a stress equal to 0%, 10%, 30%, 50% and 70% of the yield strength of the housing unit of UCF-216 ( $\sigma_{yUCF-216}$ ), and these were solved separately.

$$F_{cf} = \% \times \sigma_y \times \frac{\pi d^2}{4} \quad (1)$$

Where  $F_{cf}$ , %,  $\sigma_y$  and  $d$  were ABCF, the percentage of the desired stress value to be created on the UCF-216 housing unit, yield strength of UCF-216 housing unit and diameter of bolt, respectively. Therefore, the different ABCFs applied to the bolts were calculated by the ratio of the stress value created on the UCF-216 housing unit to the yield stress of UCF-216 housing unit ( $\sigma_{ABCF}/\sigma_{yUCF-216}$ ), based on the area where the bolt head contacts the UCF-216 housing unit surface. Bolt pretension values applied to

the bolts were given in Table 2. Also as seen in Table 2, these ABCF values were converted to bolt tightening torque using Equation 2 [18,19]. These bolt tightening torque values were the values that should be used when tightening the bolts using a torque meter.

$$T = k \times F_{cf} \times d \times l \quad (2)$$

Where  $T$ ,  $k$  and  $l$  were tightening torque, constant that depends on the bolt material and size and lubrication factor (%), respectively. The assembly process of UCF-216 housing unit to the CBBM is usually done using uncoated bolts and without the use of lubricant. Therefore, in this study, the  $k$  value was taken as 0.2. In addition, the lubrication factor was neglected.

Table 2. Applied bolt pretension and bolt tightening torque values.

$\sigma_{ABCF}/\sigma_{yUCF-216}$ (%)	Bolt pretension (N)	Bolt tightening torque (Nm)
0	0	-
10	19746	87
30	59237	261
50	98728	435
70	138220	609

## 2.5. Analyzes

Macrostructural analyses were carried out to investigate the failure mechanism in the UCF-216 housing unit. For this, first of all, it was investigated whether there was a macrostructural defect during production on a randomly selected and unused UCF-216 bearing system. Then, the fractured surface of UCF-216 housing unit, which was damaged during working on the CBBM, was examined macrostructurally. In this study, deformation stress and fatigue analyses were carried out under given boundary conditions by using static structural module of Ansys finite element software. Since the aim of this study was to determine the failure mechanism in the UCF-216 bearing, the focus was on the housing unit of UCF-216 in the analysis of the deformation, stress and fatigue safety factor distributions. During the analyses, the ambient temperature was set to 22 °C. In addition to the 10000 N load acting on the system, the effect of different bolt pretensions was also analyzed. Especially, the maximum equivalent (von-Mises) stress and minimum fatigue safety factor values and their distributions in the UCF-216 housing unit were analyzed in detail. Fatigue analysis was performed according to Goodman stress theory.

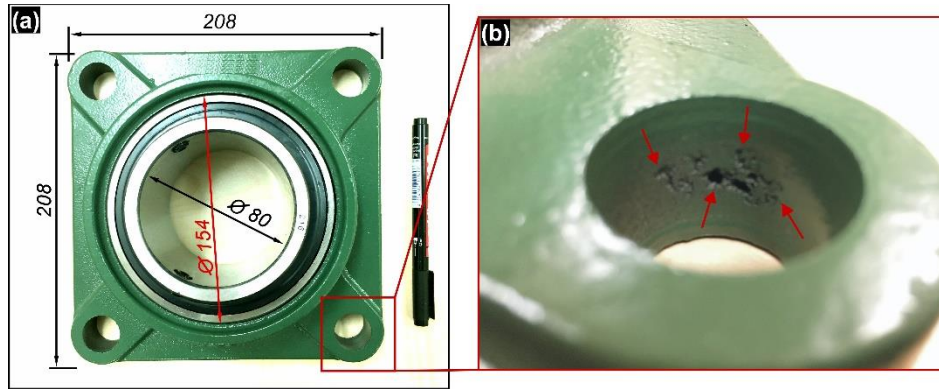


Figure 4. (a) photograph of a new and unused UCF-216, and (b) casting defects (porosities) on the inner surface of the bolt hole of this UCF-216.

### 3. Results and Discussion

#### 3.1. Macrostructural analyses

Figure 4 (a) shows a macro photograph of an unused and randomly selected UCF-216 bearing. As can be seen from the photograph in the figure, any defects could be seen on the UCF-216 housing unit when viewed in general. However, when examined in detail, it was seen that there were voids having different diameters changing in between 4 and 1 mm on the inner surface of one of the bolt holes (indicated by arrows in Figure 4 (b)). Also, the voids had irregular shapes. These voids are thought to be casting cavities (defects) formed during the manufacture of UCF-216 housing unit. Dorula et al [20] produced and studied irregularly shaped macroporosities in grey cast iron and determined that these were the result of shrinkage. The macroporosities observed by the researchers in grey cast iron were similar to the voids found in the bolt hole of UCF-216 housing unit in this study. Therefore, it was concluded that voids found on the inner surface of the bolt hole of UCF-216 housing unit occurred due to shrinkage during crystallization and solidification of cast iron. In this case, the use of appropriate inoculants has an important place in solving the problem. However, the voids were also likely to be gas porosity defects. The problem in this case could have been eliminated by using molding sand having high gas permeability or by removing excess moisture from the molding sand or by ensuring that the molding sand was not over rammed [21].

As a result, finding casting defects in mounting bolt holes of UCF-216 housing unit is a major problem; they have a notch effect, negatively affecting the mechanical properties and especially the fatigue strength. In Figure 5 (a), the macrostructure of UCF-216, which was damaged during operation in the CBBM, was given. The housing unit was broken in one of the bolt holes. In addition, when examined in general, it is seen that the damage did not cause a large number of broken pieces. The UCF-216 housing unit was broken in only two pieces. This could be

evidence that the damage was not caused by a force acting as an impact, but by a statically acting force. In addition, the fact that the failure occurred in the bolt hole region was proof of our theories of both casting defect and abnormal bolt tightening torque. Because, as indicated by the white arrows in Figure 5 (b), the damage probably caused by over-tightening the bolt was clearly noticeable. These damages were formed in the areas where the bolt contacted the housing unit and progressed into the bolt hole. Moreover, areas of porosity thought to be casting defects were also observed in Figure 5 (b) (shown in blue circle in Figure 5 (b)). Moreover, beach marks and macrocracks, which were thought to have occurred due to fatigue, were seen in Figure 5 (c). The rough and dimple-like morphology of these macrostructures was a sign that ductile fracture was dominant in the failure. Rihan [22] and Cullin [23] studied the fatigue failure of cast irons under stress and corrosion in different studies. Researchers observed fracture surface macrostructures having ductile fracture traces similar to those in this study.

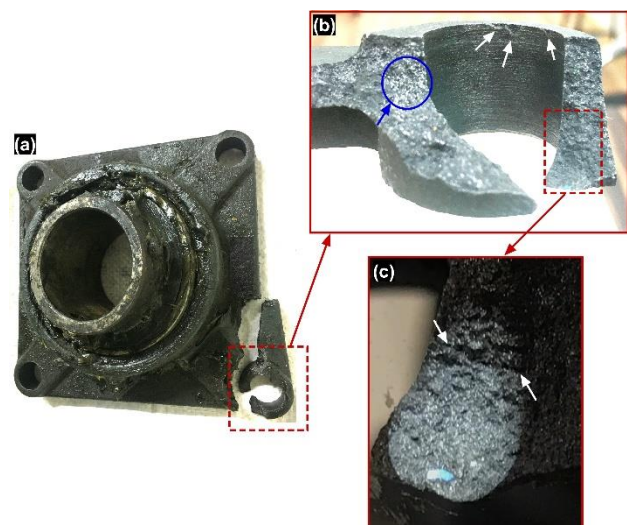


Figure 5. (a) Fracture in the housing unit of UCF-216, (b) general macrostructure of the broken piece, (c) traces of ductile fracture and fatigue failure.

3.2. Stress and fatigue analyses

As a result of different bolt pretensions applied to the bolts, the maximum von-Mises stress values on the UCF-216 ranged from 32.29 to 265.57 MPa. The graphical representation of these values were given in Figure 6.

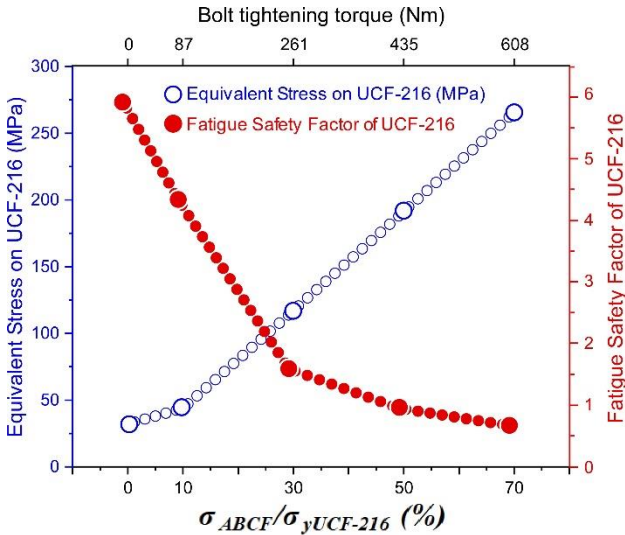


Figure 6. Graph of max. equivalent (von-Mises) stress and fatigue safety factor vs  $\sigma_{ABCF}/\sigma_{yUCF-216}$  (%) and bolt tightening torque.

Since all of these values were below the yield stress value of UCF-216, it was understood that the load applied to the system (10000 N) and the pretensions applied to the bolts (19746 – 138220 N) did not pose a problem on the UCF-216 in terms of static stress safety. When the factor of safety for stress (FOSS) coefficients obtained by dividing the yield stress of UCF-216 to the maximum von-

Mises stress occurring on the UCF-216 under the specified conditions were calculated, it was understood that the lowest FOSS value was 1.24. However, this situation was valid for the materials that did not have manufacturing defects. As shown under heading 3.1 in this study, it will be almost impossible to calculate the FOSS values correctly in case of manufacturing defects such as casting voids in the UCF-216 body.

On the other hand, von-Mises stress distributions on the UCF-216 were given in Figure 7. Figure 7 (a) shows the stress distributions in the system without bolt pretension. As can be seen, the maximum stresses were concentrated on the bolts due to the shear effect. Because, as described in section 2.4, the contact surfaces were defined as frictional contact in the assembly process of UCF-216 to the headstock surrounded by fixed support. Furthermore, as seen in Figure 7 (b), the maximum stress on UCF-216 was 32.89 MPa without applying bolt pretensions to the bolts, and the stresses were concentrated in the bolt hole near the bolt head. When the bolts were tightened enough to create 10% of the yield stress of UCF-216 (19746 N) on the UCF-216, it was observed that the maximum stress on the UCF-216 was concentrated on the bolt hole interior surface (see Figure 7 (c)). As seen in Figure 7 (d-e), the regions where stresses were most intense in UCF-216 with the increase of applied bolt pretension were again the surfaces of the bolt hole near the bolt head. Therefore, the areas with the highest risk of fracture in UCF-216 were those close to the bolt holes. As explained in the previous section, in UCF-216, the region where the fracture occurred was the same as the regions where the maximum stresses were concentrated.

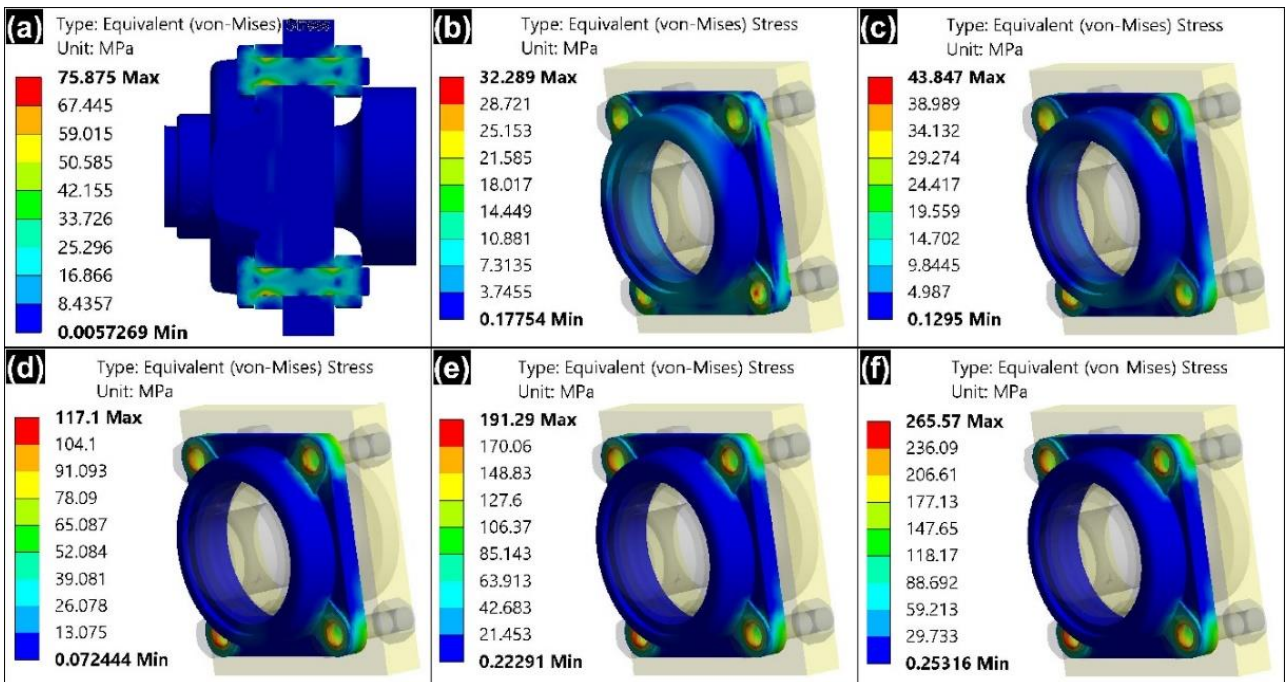


Figure 7. Distribution of equivalent (von-Mises) stress for different bolt pretensions (a) 0 N (for all components of system), (b) 0 N (for UCS-216), (c) 19746 N, (d) 59237 N, (e) 98728 N and (f) 138220 N.

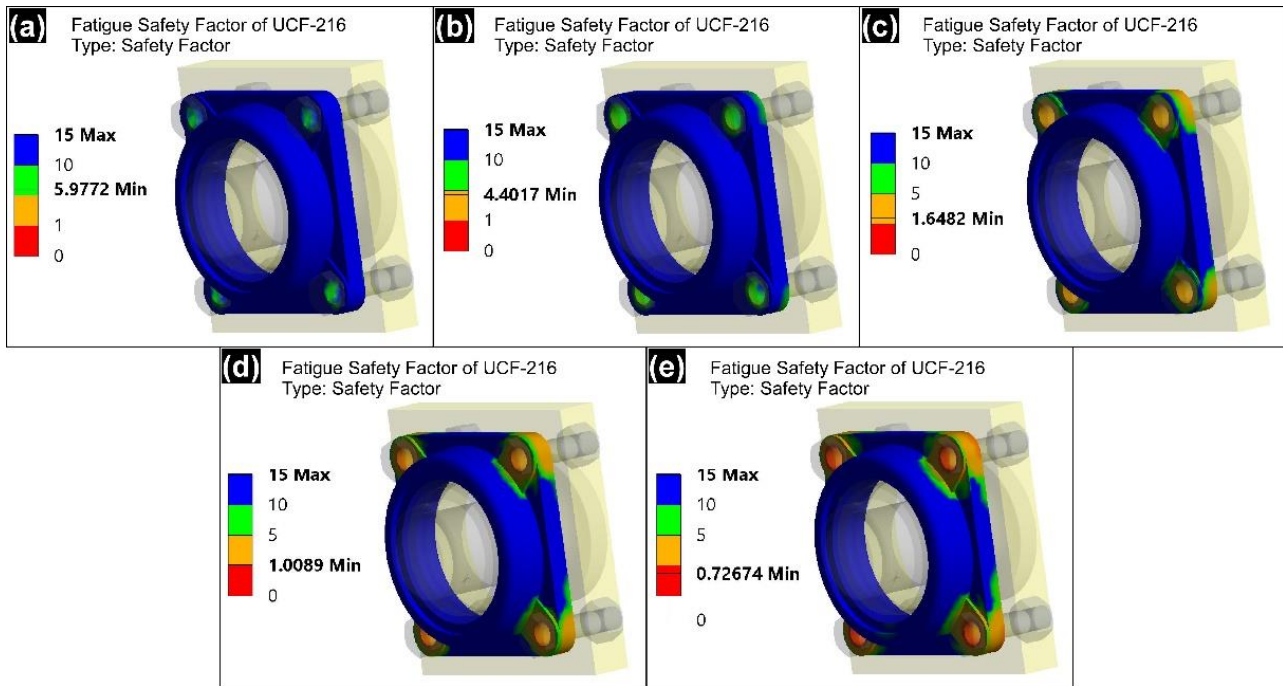


Figure 8. Distribution of fatigue safety factor for different bolt pretensions; (a) 0 N, (b) 19746 N, (c) 59237 N, (d) 98728 N and (e) 138220 N.

However, as seen in Figure 8 (e), when the bolt pretension was increased to 138220 N, the minimum FOSF value decreased to 0.73. As it is known, if the FOSF value is below 1, the system does not have an infinite cycling life. In order to use the system safely, a maximum bolt pretension of 98728 N should be applied to the UCF-216 bolts (Figure 8 (d)). This meant that the stress created by the bolts in UCF-216 could be a maximum of 50% of the yield strength of UCF-216. In one study [24], researchers demonstrated that axial force from over-tightening causes deformation and fatigue damage in cylindrical roller bearings. At the same time, previous study [17,25] had also shown that excessive bolt pretension could cause premature fatigue damage in the material. On the other hand, the presence of manufacturing defects in the material will seriously and negatively affect the fatigue life of material. Stress will intensify in the regions where casting voids exist, and these voids will be the places where fatigue cracks start and propagate by showing notch effect in cyclic loading. Therefore, the risk of failure was significantly increased, when the UCF-216 had manufacturing defects such as casting voids, as in this study.

#### 4. Conclusions

In this study, failure analysis of cast iron housing unit of an UCF-216 bearing used in a CBBM was performed. Unused and damaged UCF-216 housing units were macrostructurally examined and finite element modelling of their use in the CBBM was made by applying different bolt pretensions. Obtained results and recommendations were given in below.

- The cast iron housing of the unused UCF-216 contained casting defects. These casting defects were voids ranging from 4 to 1 mm in diameter and were on the inner surfaces of the bolt hole.
- Traces of damage caused by over-tightening were seen on the broken housing unit. In addition, both casting defects (voids) and beach marks of fatigue failure were observed in the macrostructure of the fractured surface.
- As a result of the finite element analysis, the highest von-Mises stress on the housing unit was found to be 265.57 MPa. Also, in all cases, stresses were concentrated in the bolt hole regions where failure occurred.
- It was concluded that the stress to be created on the UCF-216 housing unit by tightening the bolts can be up to 50% of the yield strength of the housing unit. The fatigue safety factor value became less than "1" when the bolts were tightened further. Minimum fatigue safety factor values were also concentrated in the bolt hole regions.
- Failure to the UCF-216 housing unit was caused by over-tightening of the bolts and casting defects also contributed.
- Appropriate inoculants could be used to eliminate casting defects from shrinkage. Moreover, casting defects caused by gas porosities could be eliminated by using molding sand having high gas permeability, by removing excess moisture from the molding sand or by ensuring that the molding sand is not compressed too much.

- The use of a torque-meter was essential when tightening the bolts

### Declaration

The authors declared no potential conflicts of interest with respect to the research, authorship, and/or publication of this article. The authors also declared that this article is original, was prepared in accordance with international publication and research ethics, and ethical committee permission or any special permission is not required.

### Author Contributions

Mustafa Guven Gok: Writing, Finite Element Analyses, Visualization, Macrostructural Analyses, Review & Editing. Mehmet Bunyamin Sahin: Writing, Investigation of the industrial application where the UCF is used.

### References

1. Starovoytova, M.D., Namango, S.S., Arusei, D., *Innovative Conceptual Design of Manual-Concrete-Block-Making-Machine*. Innovative Systems Design and Engineering, 2016. **7**(7): p. 41–52.
2. Yemane Zemicheal., Qi Houjun., *Design, Analysis and Development of Improved Hollow Concrete Block Making Machine*. International Journal of Engineering Research and Technology, 2020. **9**(03): p. 298–302.
3. Onyeakpa, C., Onundi, L., *Improvement on the Design and Construction of Interlocking Blocks and its Moulding Machine*. IOSR Journal of Mechanical and Civil Engineering, 2014. **11**(2): p. 49–66.
4. Hall, J.P., *The Early Developmental History of Concrete Block in America*. Ball State University, Historic Preservation, Master Thesis. 2009: p. 1-73.
5. Palmer, H.S., *Machine for Molding Hollow Concrete Building Blocks*. United States Patent Office, 1903. Patent No: 727,427.
6. Charles, P., *Practical Concrete-Block Making*. 1908. USA: New York Industrial Publication Company.
7. E. Catalogue. [cited January 9, 2023]; Available from: <https://www.esermakmakina.com/katalog.html>.
8. Guyer, R.A., *Rolling bearings handbook and troubleshooting guide*. 1996. USA: Radnor, Pennsylvania: Chilton Book Co.
9. Riduttori, B.S. p. A., *Gear Motor Handbook*. 1995. Berlin: Heidelberg: Springer.
10. Harris, T.A., Kotzalas, M.N., *Essential Concepts of Bearing Technology*. 2006. 6th ed., USA: Boca Raton, CRC Press.
11. Yakur, R., Çiftçi, Ö., *Investigation of the microstructure, hardness, and compressive properties of TaC-reinforced lamellar graphite cast irons*. European Mechanical Science, 2023. **7**(2): p. 56–62.
12. Yakut, R., *Investigation of Mechanical Properties of Grey Cast Irons Reinforced with Carbon Titanium Nitride (TiNC)*. Lubricants, 2023. **11**(454): p. 1–12.
13. Properties and characteristics of grey cast iron. [cited January 9, 2023]; Available from: <https://www.zhycasting.com/properties-and-characteristics-of-grey-cast-iron/>.
14. Ragul, G., Kalivarathan, G., Jayakumar, V., Maruthur, P., Jacob, I., Naveen Kumar, S., *An Analytical Investigation On Design And Structural Analysis Of Cam Shaft Using Solid Works And Ansys In Automobiles*. Indian Journal of Science and Technology, 2016. **9**(36): p. 1–9.
15. Kováčiková, P., Bezdedová, R., Vavro, J., Vavro, J., *Comparison of numerical analysis of stress-strain states of cast iron with vermicular graphite shape and globular graphite shape*. Procedia Engineering, 2016. **136**(): p. 28–32.
16. Chaturvedi, E., Dwivedi, R., *Design and Static Load Analysis Comparing Steel, Grey Cast Iron and Titanium Alloy as Materials for Breech Hinged Lugs in Recoil Weapons*. Advances in Military Technology, 2018. **13**(2): p. 265–75.
17. Gok, M.G., Cihan, O., *Investigation of Failure Mechanism of a DCI Engine Connecting Rod*. European Journal of Technique, 2021. **11**(2): p. 222–228.
18. Yu, Q., Zhou, H., Wang, L., *Finite element analysis of relationship between tightening torque and initial load of bolted connections*. Advances in Mechanical Engineering, 2015. **7**(5): p. 168781401558847.
19. Mínguez, J.M., Vogwell, J., *Effect of torque tightening on the fatigue strength of bolted joints*. Engineering Failure Analysis, 2006. **13**(8): p. 1410–1421.
20. Dorula, J., Kopyci, D., Guzik, E., Szczesny, A., *Procedure of Eliminating Porosity in Grey Cast Iron with Low Sulphur Content*. Materials, 2022. **15**(6273): p. 1–20.
21. Sertucha, J., Lacaze, J., *Casting Defects in Sand-Mold Cast Irons—An Illustrated Review with Emphasis on Spheroidal Graphite Cast Irons*. Metals, 2022. **12**(3): p. 1–80.
22. Rihan, R., Raman, R.K.S., Ibrahim, R.N., *Circumferential notched tensile (CNT) testing of cast iron for determination of threshold (KISCC) for caustic crack propagation*. Materials Science and Engineering A, 2005. **407**(1): 207–212.
23. Cullin, M.J., Petersen, T.H., Paris, A., *Corrosion Fatigue Failure of a Gray Cast Iron Water Main*. Journal of Pipeline Systems Engineering and Practice, 2015. **6**(2): p. 5014003.
24. Hou, X., Diao, Q., Liu, Y., Liu, C., Zhang, Z., Tao, C., *Failure Analysis of a Cylindrical Roller Bearing Caused by Excessive Tightening Axial Force*. Machines, 2022. **10**(5): p. 1–15.
25. Witek, L., Zelek, P., *Stress and failure analysis of the connecting rod of diesel engine*. Engineering Failure Analysis, 2019. **97**(): p. 374–82.